

NLRP6 Inflammasome Orchestrates the Colonic Host-Microbial Interface by Regulating Goblet Cell Mucus Secretion

Marta Wlodarska,^{1,2} Christoph A. Thaiss,³ Roni Nowarski,⁴ Jorge Henao-Mejia,⁴ Jian-Ping Zhang,⁵ Eric M. Brown,^{1,2} Gad Frankel,⁶ Maayan Levy,³ Meirav N. Katz,^{3,7} William M. Philbrick,⁵ Eran Elinav,^{3,10,*} B. Brett Finlay,^{1,2,8,10,*} and Richard A. Flavell^{4,9,10,*}

¹Michael Smith Laboratories, The University of British Columbia, Vancouver, BC V6T 1Z4, Canada

²Department of Microbiology and Immunology, University of British Columbia, Vancouver, BC V6T 1Z4, Canada

³Immunology Department, Weizmann Institute of Science, Rehovot 76100, Israel

⁴Department of Immunobiology, Yale University School of Medicine, New Haven, CT 06520, USA

⁵Center on Endocrinology and Metabolism, Yale University School of Medicine, New Haven, CT 06520, USA

⁶MRC Center for Molecular Bacteriology and Infection, Department of Life Sciences, Flowers Building, Imperial College, London SW7 2AZ, UK

⁷Research Center for Digestive Tract and Liver Diseases, Tel Aviv Sourasky Medical Center, Sackler Faculty of Medicine, Tel Aviv University, Tel Aviv 64239, Israel

⁸Department of Biochemistry and Molecular Biology, University of British Columbia, Vancouver, BC V6T 1Z4, Canada

⁹Howard Hughes Medical Institute, Chevy Chase, MD 20815, USA

¹⁰These authors contributed equally to this work and are listed alphabetically

*Correspondence: eran.elinav@weizmann.ac.il (E.E.), bfinlay@interchange.ubc.ca (B.B.F.), richard.flavell@yale.edu (R.A.F.)

<http://dx.doi.org/10.1016/j.cell.2014.01.026>

SUMMARY

Mucus production by goblet cells of the large intestine serves as a crucial antimicrobial protective mechanism at the interface between the eukaryotic and prokaryotic cells of the mammalian intestinal ecosystem. However, the regulatory pathways involved in goblet cell-induced mucus secretion remain largely unknown. Here, we demonstrate that the NLRP6 inflammasome, a recently described regulator of colonic microbiota composition and biogeographical distribution, is a critical orchestrator of goblet cell mucin granule exocytosis. NLRP6 deficiency leads to defective autophagy in goblet cells and abrogated mucus secretion into the large intestinal lumen. Consequently, NLRP6 inflammasome-deficient mice are unable to clear enteric pathogens from the mucosal surface, rendering them highly susceptible to persistent infection. This study identifies an innate immune regulatory pathway governing goblet cell mucus secretion, linking nonhematopoietic inflammasome signaling to autophagy and highlighting the goblet cell as a critical innate immune player in the control of intestinal host-microbial mutualism.

INTRODUCTION

Inflammasomes are cytoplasmic multiprotein complexes that are expressed in various cell lineages and orchestrate diverse functions during homeostasis and inflammation. The complexes are composed of one of several NLR proteins, such as NLRP1,

NLRP3, NLRC4, and NLRP6, which function as innate sensors of endogenous or exogenous stress or damage-associated molecular patterns. NLRP6 is an NLR protein that has been shown to participate in inflammasome signaling (Grenier et al., 2002) and to play critical roles in defense against infection, auto-inflammation, and tumorigenesis (Anand et al., 2012; Chen et al., 2011; Elinav et al., 2011b; Hu et al., 2013; Normand et al., 2011). NLRP6 is highly expressed in the intestinal epithelium (Chen et al., 2011; Elinav et al., 2011b; Normand et al., 2011), but the signal(s) and mechanisms leading to NLRP6 downstream effects remain elusive.

It is becoming clear that NLRP6 plays critical roles in maintaining intestinal homeostasis and a healthy intestinal microbiota. NLRP6 is essential for mucosal self-renewal and proliferation, rendering NLRP6-deficient mice more susceptible to intestinal inflammation and to chemically induced colitis as well as increased tumor development (Chen et al., 2011; Normand et al., 2011). Further contributing to intestinal health, NLRP6 participates in the steady-state regulation of the intestinal microbiota, partly through the basal secretion of IL-18 (Elinav et al., 2011b). NLRP6 deficiency leads to the development of a colitogenic microbiota that is intimately associated at the base of the colonic crypt, stimulating a proinflammatory immune response, ultimately leading to increased susceptibility to chemically induced colitis in NLRP6-deficient mice (Elinav et al., 2011b). However, the mechanisms by which the absence of a single inflammasome component leads to changes in intestinal microbial community composition and biogeographical distribution remain unknown.

Microbial dysbiosis and the increased susceptibility to DSS-induced colitis in NLRP6-deficient mice suggest that NLRP6 may play an important role in intestinal barrier maintenance. The primary defense against microbial and pathogen penetration into the lamina propria is the single layer of epithelial cells and its

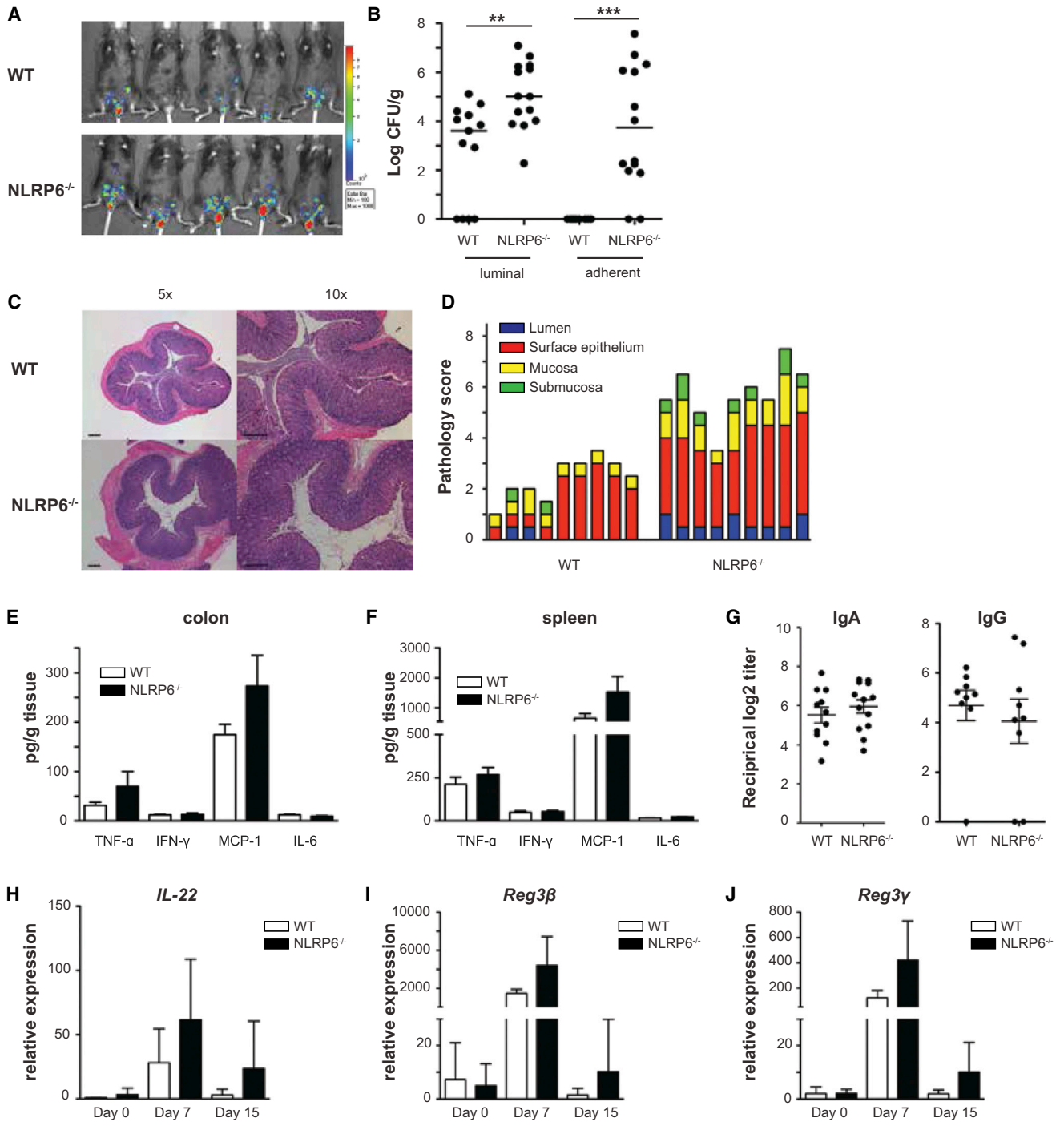


Figure 1. NLRP6 Protects from Enhanced Enteric Infection

WT and *Nlrp6*^{-/-} mice were infected with 10⁹ cfu of bioluminescent *C. rodentium* and analyzed on day 15 p.i., unless otherwise stated. (A) In vivo whole body bioluminescence imaging of WT and *Nlrp6*^{-/-} mice on day 9 p.i. show increased bacterial growth in *Nlrp6*^{-/-} mice. (B) Both luminal (fecal matter) and adherent (extensively washed colons) bacterial colonization is enhanced in *Nlrp6*^{-/-} mice. Results are pooled from two separate experiments, n = 12–14 per group. Significance determined using the Mann-Whitney U-test and expressed as the median (**p ≤ 0.0033; ***p < 0.0001). (C) H&E-stained distal colon sections from WT and *Nlrp6*^{-/-} mice show an increase in inflammation and crypt ulceration throughout the mucosa of *Nlrp6*^{-/-} mice. Magnification = 5×, 10×. The scale bar represents 200 μm. (D) Histopathology scores from distal colon tissues of *Nlrp6*^{-/-} and WT mice. Each bar represents one individual mouse and shows scores for damage to the submucosa, mucosa, surface epithelium, and lumen, n = 9 per group.

(legend continued on next page)

associated protective mucus layer. Goblet cells (GC), specialized intestinal epithelial cells, produce and secrete mucins, predominantly Muc2, into the intestinal lumen, thereby forming the mucus layer (Tytgat et al., 1994). Muc2 biosynthesis involves protein dimerization in the ER, glycosylation in the Golgi apparatus, oligomerization, and dense packing of these large net-like structures into secretory granules of the goblet cell (Ambort et al., 2012). Mucin-containing granules are stored within a highly organized array of microtubules and intermediate filaments called the theca, which separates mucin granules from the rest of the cytoplasm and gives mature goblet cells their distinctive shape (Forstner, 1995). Exocytosis of mucin occurs when apically oriented mucin granules fuse with the plasma membrane in a complex but not understood process (Ambort et al., 2012; Forstner, 1995). The resultant intestinal mucus layer consists of two stratified layers and plays a key role in the maintenance of intestinal homeostasis; it protects the epithelium from dehydration, physical abrasion, and commensal and invading microorganisms (Johansson et al., 2008; Linden et al., 2008). In contrast to the loose matrix and microbiota containing outer mucus layer, the inner mucus layer composition is dense and devoid of the microbiota (Johansson et al., 2008), and functions as a barrier, which serves to minimize microbial translocation and prevent excessive immune activation. Muc2-deficient mice, which lack a normal intestinal mucus layer, are more susceptible to intestinal inflammation and infection, stemming from heightened commensal or pathogenic microbial interaction with the epithelial layer (Gill et al., 2011; van der Sluis et al., 2006, 2008). Muc2 deficiency leads to exacerbated disease by the attaching and effacing (A/E) pathogen, *Citrobacter rodentium*, characterized by an increased rate of pathogen colonization and an inability to clear pathogen burdens through increased mucus secretion (Bergstrom et al., 2010).

In this study, we describe a mechanism by which NLRP6 inflammasome simultaneously influences intestinal barrier function and microbial homeostasis, through regulation of goblet cell mucus secretion. In mice that are deficient for NLRP6, ASC, or caspase-1, mucin granule exocytosis and resultant mucus layer formation by goblet cells is impaired, leading to increased susceptibility to enteric infection. Mechanistically, NLRP6 deficiency leads to abrogation of autophagy in goblet cells, providing a link between inflammasome activity, autophagy, mucus granule exocytosis, and antimicrobial barrier function.

RESULTS

NLRP6 Inflammasome Deficiency Impairs Host-Mediated Enteric Pathogen Clearance

The NLRP6 inflammasome regulates colonic microbial ecology, and NLRP6-deficient mice show altered microbial community

composition, suggesting that NLRP6 inflammasome activity is involved in the maintenance of a stable community structure in the intestine (Elinav et al., 2011b). A major cause of microbial community disruption in the intestine is enteric infection. Mice infected with *C. rodentium* or *Salmonella enterica* undergo massive changes in microbiota composition (Lupp et al., 2007; Stecher et al., 2007). To analyze whether NLRP6 plays a role in host defense against enteric infections, we tested the ability to clear *C. rodentium* by NLRP6-deficient mice. We used a bioluminescent variant of *C. rodentium* that allows for noninvasive in vivo monitoring of bacterial growth over the time course of the infection (Wiles et al., 2006). Remarkably, at day 9 postinfection (p.i.), *Nlrp6*^{-/-} mice were extensively colonized with *C. rodentium* when compared to wild-type (WT) mice (Figure 1A). Total *C. rodentium* luminal (fecal matter only) and adherent (washed intestinal tissue only) burden of the large intestine were also significantly higher in *Nlrp6*^{-/-} mice at day 15 p.i. when compared to WT mice (Figure 1B). This trend was reproducible regardless of the source of C57Bl mice (data not shown). Strikingly, at this late time point, 86% of the *Nlrp6*^{-/-} mice still had *C. rodentium* attached to the intestinal epithelium, in contrast to 0% of WT mice (Figure 1B). *Nlrp6*^{-/-} mice also showed a significant increase in pathology in the distal colon at day 15 p.i. (Figure 1C), confirming the high intestinal burdens of *C. rodentium*. This increase in pathology was characterized by greater submucosal edema, more extensive damage to the surface mucosa and ulceration, and extensive regions of mucosal hyperplasia (Figure 1D). The increased *C. rodentium* burden and pathology at day 15 p.i. was not accompanied by decreased production of proinflammatory cytokines in the colon or spleen (Figures 1E and 1F, respectively), *C. rodentium*-specific antibody profile (Figure 1G), or impaired signaling through the IL-22 pathway and its related downstream antimicrobial peptides (Figures 1H–1J). Likewise, colonic IL-1 β and IL-18 mRNA levels were similar in naive and infected WT and *Nlrp6*^{-/-} mice (Figures S1A and S1B available online). Intestinal neutrophil and T cell numbers, as measured by myeloperoxidase and CD90.1 immunohistochemistry, respectively, were reactively elevated in *Nlrp6*^{-/-} as compared to WT mice (Figures S1C and S1D). This suggested that increased bacterial colonization in *Nlrp6*^{-/-} mice was not a result of an ineffective immune response to the pathogen, but rather by an alternate nonhematopoietic cell-mediated mechanism.

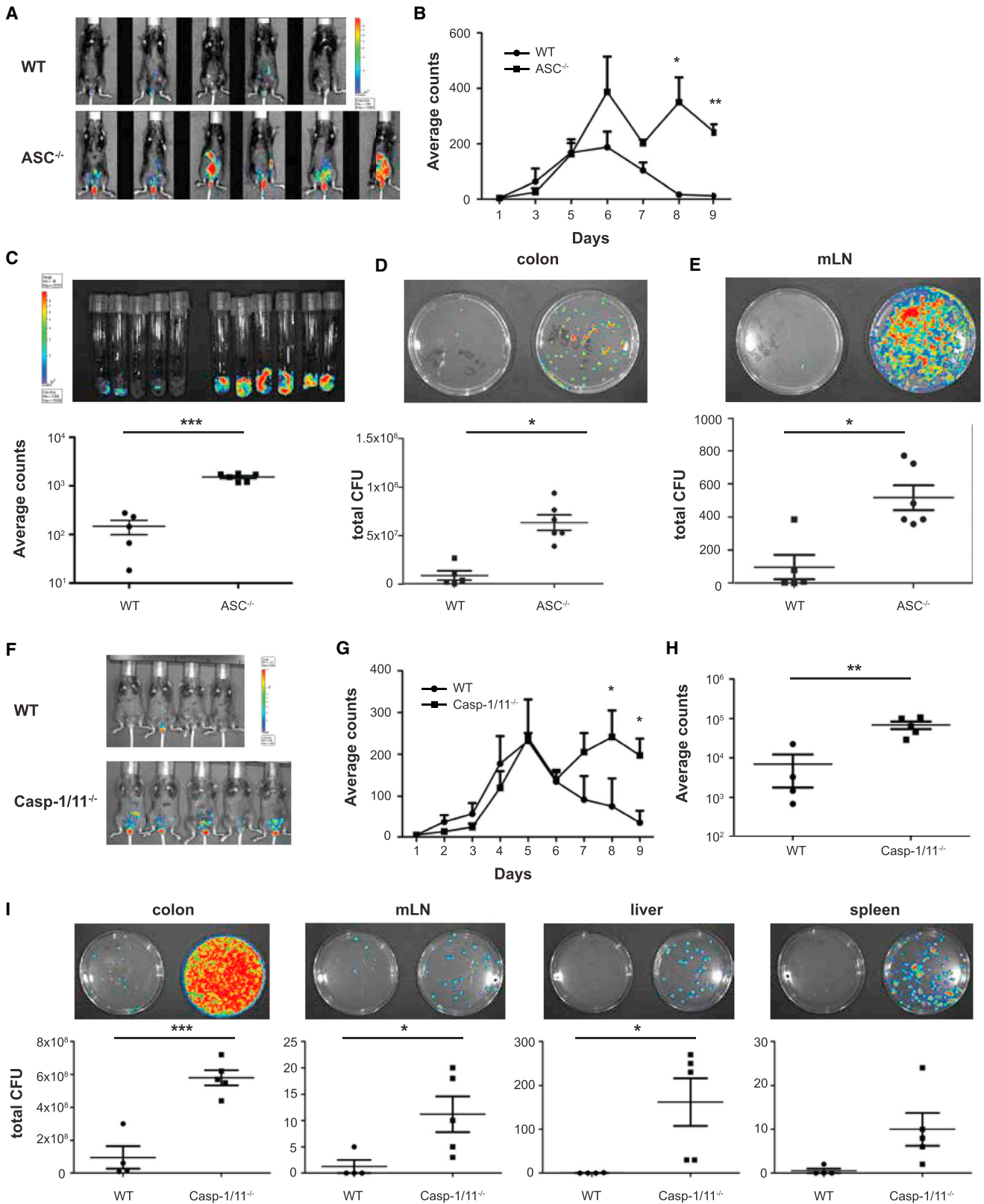
To determine whether an NLRP6 inflammasome was necessary for host defense to *C. rodentium*, we studied mice deficient in ASC and caspase-1 for their ability to clear *C. rodentium* infection. Like *Nlrp6*^{-/-}, *Asc*^{-/-} and *Caspase-1/11*^{-/-} mice were unable to clear *C. rodentium* from the colon and remained highly colonized while WT mice began to clear infection at day 9

(E and F) Secretion of proinflammatory cytokines in the colon (E) and spleen (F) is unchanged between WT and *Nlrp6*^{-/-} mice. Results are pooled from two separate infections of WT and *Nlrp6*^{-/-} mice, n = 13 and 14, respectively. Significance determined using two-tailed Student's t test and expressed as the mean \pm SEM.

(G) *C. rodentium*-specific colonic IgA and systemic IgG titers. Results are pooled from two separate experiments, n = 9–13 per group.

(H–J) Quantitative RT-PCR showing expression of IL-22 (H), *Reg3 β* (I), and *Reg3 γ* (J) relative to *gapdh* in the distal colon of WT and *Nlrp6*^{-/-} mice over the course of *C. rodentium* infection, n = 4–9. Significance determined using two-tailed Student's t test and expressed as the mean \pm SD.

See also Figure S1.



(legend on next page)

p.i. (Figures 2A, 2B, and 2F–2H). As a result, mice lacking any inflammasome component featured enhanced colonic and systemic colonization with *C. rodentium* (Figures 2C–2E and 2I). Collectively, these results suggested that NLRP6 inflammasome activation is pivotal for host defense against A/E pathogen infection.

NLRP6 Contributes to Intestinal Homeostasis through Regulation of Goblet Cell Function

To understand the mechanism by which NLRP6 inflammasome activity contributes to host defense to enteric infection, we sought to identify the cell type mediating this antipathogen response. We have previously shown that NLRP6 is highly expressed within the nonhematopoietic intestinal compartment, especially within intestinal epithelial cells (Elinav et al., 2013a, 2011b). This near-exclusive contribution of colonic epithelial cells to intestinal NLRP6 expression was maintained during *Citrobacter* infection, as measured by high purity sorting of epithelial and hematopoietic colon cells during day 10 of infection (Figure 3A). However, these cells can be further divided based on morphologic and functional differences into various subsets, including enterocytes, goblet cells, Paneth cells, and intestinal stem cells. To begin our investigation of the cellular source of NLRP6 activity, we performed a series of in situ hybridization studies on colonic sections from WT, ASC^{-/-}, and *Nlrp6*^{-/-} mice. We found NLRP6 to be highly expressed throughout the intestinal mucosa of WT mice, concentrated in the apical mucosal region (Figure 3B, upper panel), specifically in goblet cells, seen as extensive probe binding in areas surrounding the theca containing mature mucin granules (Figure 3B, lower panel). Intestines deficient in the adaptor protein, ASC, show similar NLRP6 expression and localization pattern (Figure 3C), whereas *Nlrp6*^{-/-} mice remained negative to this staining (Figure 3D). This expression pattern of NLRP6 suggested that NLRP6 contribute to mucosal defense by regulating goblet cell function and mucus production.

Mucus secretion is critically important in host defense against multiple enteric pathogens, including the A/E family of pathogens that adhere to the host surface epithelial layer where they perform their pathogenic functions (Gill et al., 2011). As an important line of defense, the host utilizes mucus secretion as a method to prevent attachment and remove the adherent load from the mucosal surface (Bergstrom et al., 2010). To explore whether defective goblet cell-mediated mucus secretion was indeed responsible for the enhanced susceptibility of NLRP6 inflammasome-deficient mice to enteric infection, we sought to characterize goblet cell function in *Nlrp6*^{-/-} inflammasome-deficient

and WT mice. Intriguingly, we found that the intestinal epithelium of *Nlrp6*^{-/-}, *Asc*^{-/-}, and *Caspase 1/11*^{-/-} mice lack a thick continuous overlying inner mucus layer (Figures 4A and 4B; “i,” inner mucus layer) and exhibit a marked goblet cell hyperplasia (Figures 4A and 4C), suggesting a dramatic functional alteration in goblet cell mucus secretion in NLRP6 inflammasome-deficient mice. Further exploring this deficiency, we used transmission electron microscopy to visualize the theca of goblet cells, which is normally packed with mucin granules. In WT mice, once the theca containing mucin granules reach the apical surface of the intestinal epithelium they fuse with the epithelium, releasing the stored mucins and associated proteins into the intestinal lumen (Figure 4D, left panel). In contrast, the distal colon of *Nlrp6*^{-/-} mice featured increased accumulation of intracellular mucin granules and an apparent inability of these granules to fuse with the apical surface of the intestinal epithelium (Figure 4D, right panel). Likewise, mucus staining with the lectin *Ulex europaeus* agglutinin I (UEA-1) revealed a lack of intact mucus layer and goblet cell hyperplasia in *Nlrp6*^{-/-} intestinal sections (Figure 4E).

The abrogated mucus secretion in *Nlrp6*^{-/-} mice was expected to enable increased attachment of *C. rodentium* during infection. To address this, we performed immunostaining for the *C. rodentium*-derived infection marker translocated intimin receptor (Tir) on colon sections at day 7 p.i. as a measure of *C. rodentium* attachment to and infection of the intestinal epithelium. In the early stages of infection in WT mice, *C. rodentium* primarily infected the mucosal surface (Tir-positive) but did not invade the crypts (Figure 4F). However, in *Nlrp6*^{-/-} mice, *C. rodentium* was dramatically more invasive, penetrated deeper into the crypts and was found more frequently associated with goblet cells (Muc2-positive; Figures 4F and 4G). These results, in complete agreement with our previous results featuring commensal bacteria in close approximation to the normally near-sterile crypt base (Elinav et al., 2011b), demonstrate that NLRP6 deficiency and resultant mucus alterations, result in abnormal microbial approximation to the host mucosal surface, leading to infectious, inflammatory, metabolic, and neoplastic consequences (Chen et al., 2011; Elinav et al., 2011b; Normand et al., 2011).

To further define this observed defect in mucus secretion, transcriptional regulation of goblet cell-specific proteins including the mucins, Muc1, Muc2, Muc3, and Muc4, intestinal trefoil factor 3 (TFF-3), and resistin-like molecule β (Relmβ) was assessed. These proteins have defined roles in intestinal homeostasis; Muc2 is a gel-forming mucin and the main component of the intestinal mucus layer (Johansson et al., 2008), Muc1, Muc3, and Muc4 are surface-bound mucins with roles in signaling and

Figure 2. Inflammasome Signaling Is Required for Clearance of *C. rodentium* Infection

WT, *Asc*^{-/-}, and *Caspase-1/11*^{-/-} mice were infected with 10⁹ cfu of bioluminescent *C. rodentium* and analyzed on day 9 postinfection. (A, B, F, and G) Representative images (A and F) and time course quantification (B and G) of in vivo whole body bioluminescence imaging shows elevated bacterial growth in the intestine of *Asc*^{-/-} (A and B) and *Caspase-1/11*^{-/-} mice (F and G). Significance determined using two-tailed Student's t test and expressed as the mean ± SEM. (C and H) Ex vivo imaging of extensively washed colonic explants shows enhanced bacterial attachment to colons of *Asc*^{-/-} (C) and *Caspase-1/11*^{-/-} (H) mice. Significance determined using two-tailed Student's t test and expressed as the mean ± SEM. (D, E, and I) Bacterial plating demonstrates a higher colonic and systemic colonization of *Asc*^{-/-} (D and E) and *Caspase-1/11*^{-/-} (I) mice. Significance determined using two-tailed Student's t test and expressed as the mean ± SEM.

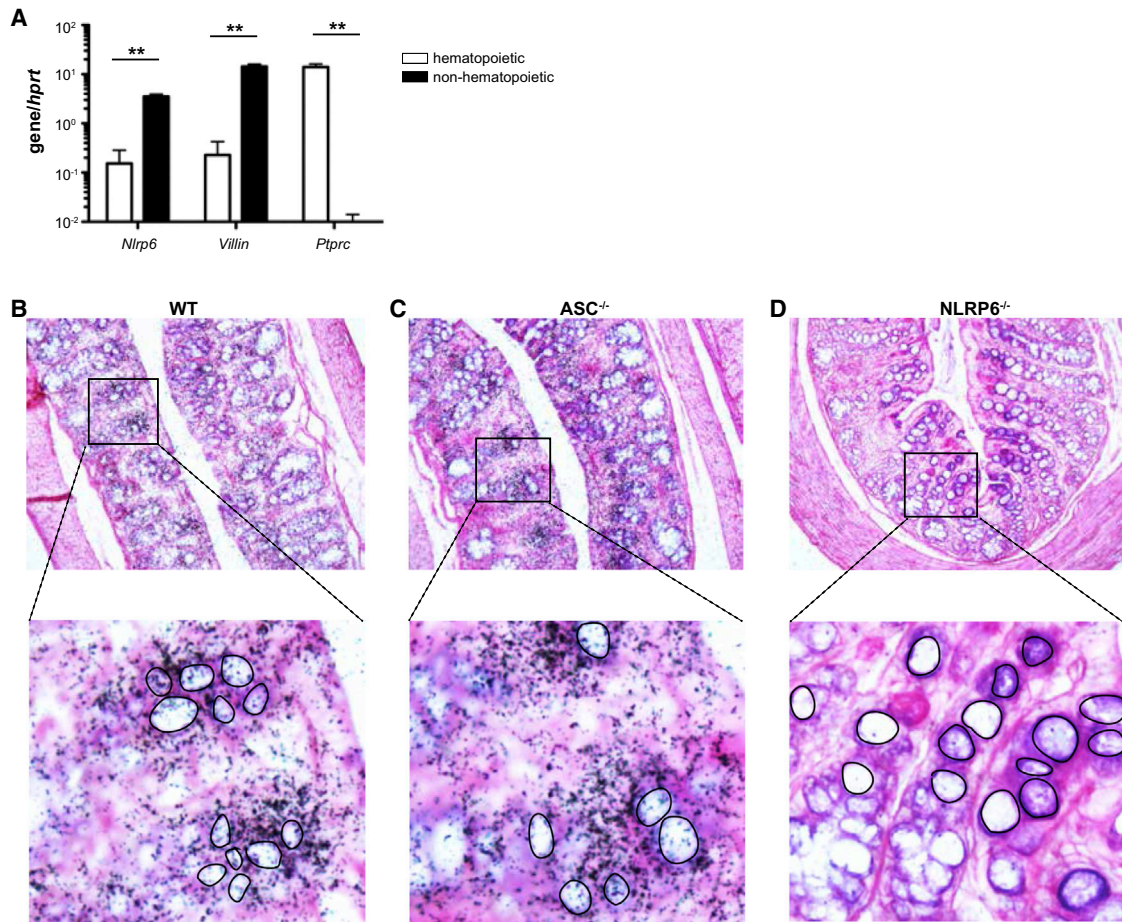


Figure 3. NLRP6 Is Expressed in Goblet Cells

(A) Analysis of NLRP6 expression during infection in sorted colonic epithelial and hematopoietic (CD45⁺) cells. The purity of the sorted populations was analyzed by RT-qPCR using *vill1* and *ptprc* as markers for epithelial and hematopoietic cells, respectively. NLRP6 expression closely mirrored that of colonic epithelial cells. Significance determined using two-tailed Student's t test and expressed as the mean \pm SEM.

(B–D) In situ hybridization with an NLRP6-specific probe, visible as black dots, with an H&E counterstain. The theca (housing all mucin-containing granules) within goblet cells is not stained with H&E and identified as unstained circles (outlined with black circles) allowing localization of goblet cells within the epithelium. (B) Representative localization of NLRP6 in a WT distal colon section, showing that staining is concentrated in the apical region of the epithelium. Magnifications demonstrate an enrichment of NLRP6 mRNA in proximity to goblet cells, seen as increased probe-binding to areas surrounding the theca of goblet cells. (C) As in (B), but in *Asc*^{-/-} mice. (D) No nonspecific probe binding is seen in *Nlrp6*^{-/-} distal colon sections.

tumorigenesis, TFF3 synergizes with Muc2 to enhance the protective properties of the mucus layer (van der Sluis et al., 2006), and Relm β has an important role in innate immunity and host defense (Artis et al., 2004; Nair et al., 2008). No reduction was seen in any goblet cell-specific protein transcript levels in *Nlrp6*^{-/-} mice (Figure S2A). In fact, Relm β expression was significantly elevated in these mice (Figure S2A). This suggests that the deficiency in mucus production in *Nlrp6*^{-/-} mice is not due to reduced transcript production.

We have recently demonstrated that NLRP6 inflammasome-deficient mice feature a distinct microbiota configuration, which drives a context-specific susceptibility to intestinal auto-inflammation, nonalcoholic fatty liver disease, and colorectal cancer, through several microbial-induced mechanisms (Elinav et al., 2011a, 2011b, 2013a, 2013b; Henao-Mejia et al., 2012, 2013a, 2013b; Hu et al., 2013). To study whether the inflammasome-

deficient microbiota is responsible for the altered steady-state goblet cell phenotype, we cohoused WT mice with *Nlrp6*^{-/-} or *Asc*^{-/-} mice. This modality induces full microbiota configuration transfer into cohoused WT mice, allowing for direct assessment of the inflammasome-deficient microbiota as compared to WT microbiota in singly housed WT mice. As is shown in Figures S2B–S2E, cohoused WT mice featured a comparable mucus layer and goblet cell hyperplasia to that of singly-housed WT mice. Similarly, WT littermate controls did not feature mucus layer disturbances (data not shown), ruling out a significant microbiota contribution to the observed goblet cell impairment in NLRP6 inflammasome-deficient mice. Likewise, the mucus layer and goblet hyperplasia was normal in *IL-1R*^{-/-} and *IL-18*^{-/-} mice (Figure S3), suggesting that the primary goblet cell defect in the absence of NLRP6 was mediated by IL-1- and IL-18-independent mechanisms.

NLRP6 Regulates Goblet Cell Mucus Granule Secretion

In addition to the lack of a continuous inner mucus layer in *Nlrp6*^{-/-} mice (Figure 5A, i), mucin granule-like structures were also found in the lumen of *Nlrp6*^{-/-} mice (Figure 5A, inset a). In several cases, these structures were densely packed in the intestinal lumen (Figure 5B, arrow). They measured 6.28 $\mu\text{m} \pm 0.80 \mu\text{m}$ in diameter (100 granules measured, data not shown) and were never found in WT mice. This width compares to the size of mucin-containing granules in mature goblet cells found in the mucosa, which measured 7.29 $\mu\text{m} \pm 2.18 \mu\text{m}$ in diameter (100 granules measured, data not shown). In order to further confirm that these structures were mucin granules, we used immunofluorescence (Figure 5C) and transmission electron microscopy (Figure 5D). Murine calcium-activated chloride channel family member 3 (mCLCA3, alias Gob-5) was previously identified as a protein exclusively associated with mucin granule membranes of intestinal goblet cells (Leverkoehne and Gruber, 2002). Immunofluorescence utilizing an anti-mCLCA3 antibody demonstrated punctate staining in the lumen of *Nlrp6*^{-/-} intestinal tissue (Figure 5C) suggesting the presence of intact mucin granules in the lumen. In contrast, WT tissue showed punctate staining at the surface of the intestinal epithelium, where mucin granules fuse with the intestinal epithelium, and some diffuse staining in the lumen (Figure 5C), as previously reported (Leverkoehne and Gruber, 2002). Transmission electron microscopy showed mucin granules protruding into the intestinal lumen with their membranes intact, with none of the granules found to fuse with or empty into the lumen. Furthermore, these intact membrane-bound structures were also present inside the lumen (Figure 5D). Utilizing scanning electron microscopy, many protruding mucin granules were observed in the intestinal epithelium of *Nlrp6*^{-/-} mice (Figure 5E, arrows), which were rarely seen in WT mice. Further, enlargement of the mucin granule protrusions clearly shows that each is made up of multiple granules (Figure 5F). It is likely that these protruding mucin granules get sloughed off into the intestinal lumen via the shearing force of fecal matter passing through the intestine explaining their luminal presence in *Nlrp6*^{-/-} mice.

To determine whether this function of NLRP6 requires recruitment of members of the classical inflammasome pathway to regulate mucus secretion, we utilized scanning (SEM) and transmissive (TEM) electron microscopy to characterize the intestinal mucus layer of *Caspase-1/11*^{-/-} and *Asc*^{-/-} mice. In agreement with the observations above, we found large intestines in *Caspase-1/11*^{-/-} and *Asc*^{-/-} mice to also feature goblet cells lacking mucus secretion. *Caspase-1/11*^{-/-} mice feature goblet cells with a weakly packed theca that upon fusion with the intestinal epithelium does not readily release contained mucin granules (Figures S4D and S4E). Similar to *Nlrp6*^{-/-} mice, *Asc*^{-/-} mice show the accumulation of densely packed goblet cells with mucus granules protruding into the intestinal lumen without mucus secretion. Findings similar to the *Nlrp6*-deficient intestinal wall were evident with scanning electron microscopy in both the *Caspase-1/11*-deficient and *Asc*-deficient intestinal epithelium (Figures S4F and S4H), suggesting that both the NLRP6 sensor and assembly of the inflammasome complex are required for appropriate mucus granule fusion with the intestinal epithelium and subsequent mucus secretion.

NLRP6 Inflammasome Is Critical for Autophagy in Intestinal Epithelial Cells

We next sought to dissect the molecular pathways by which NLRP6 inflammasome signaling regulates goblet cell mucus secretion. Paneth cells are a small intestinal secretory epithelial cell subset that has functional importance in orchestration of the host-microbial interface by secretion of a variety of host-protective mediators. Paneth cells are normally not found within the large intestine, where the much less studied goblet cells are believed to mediate many similar host-protective secretory functions. In Paneth cells, autophagy has been shown to be critical for proper function of secretory pathways (Cadwell et al., 2008). Similar autophagy-mediated regulation of secretory pathways has been described in osteoclasts (DeSelm et al., 2011) and mast cells (Ushio et al., 2011). Furthermore, a recent proteomic study demonstrated the presence of an autophagy-related protein, Atg5, in intestinal mucin granules (Rodríguez-Piñeiro et al., 2012). Moreover, mice with deletion of Atg7 in intestinal epithelial cells were recently found to feature enhanced susceptibility to *C. rodentium* infection (Inoue et al., 2012). To determine if defective autophagy provided the mechanistic link between NLRP6 deficiency, goblet cell dysfunction, and enhanced enteric infection, we crossbred NLRP6-deficient mice with transgenic mice systemically expressing GFP fused to LC3. LC3 functions as a marker protein for autophagosomes (Mizushima et al., 2004). During the formation of the autophagosome, the unconjugated cytosolic form of LC3 (called LC3-I) is converted to the phosphatidylethanolamine-conjugated (lipidated) form (called LC3-II) and incorporated to the membrane that is visible as discrete puncta using immunofluorescence analysis (Choi et al., 2013). In WT mice, the LC3-GFP signal had a characteristic punctate staining indicative of the formation of autophagosomes (Figure 6A). This LC3-GFP autophagosome staining was also localized within goblet cells (cells both Muc2- and GFP-positive; Figure 6B). Strikingly, in NLRP6-deficient intestinal tissue, the LC3-GFP signal was absent (Figures 6A and 6C). NLRP6 deficiency led to reduced levels of the LC3-GFP protein and an accumulation of p62 in isolated intestinal epithelial cells (Figures 6D and 6E), indicative of diminished autophagosome formation. Endogenous LC3-I and LC3-II levels were also severely altered in *Nlrp6*^{-/-}, *Asc*^{-/-}, and *Caspase-1/11*^{-/-} mice in intestinal epithelial cells, featuring an elevated LC3-I/LC3-II ratio and accumulation of P62 (Figures 6F–6H). An accumulation of degenerating mitochondria, described as unhealthy lacking intact cristae and containing dense inclusion bodies of proteins, in NLRP6-deficient intestinal epithelium (Figure 6I) further supported a defect in autophagy processes. Altogether, these results suggest that NLRP6 deficiency mediates profound autophagy impairment in goblet cells that, like in the functionally correlative Paneth cell, result in secretion alterations that lead to significant impairment in colonic host-microbial interactions. To definitely establish the link between inflammasome signaling and autophagy in mediating the goblet cell phenotype, we examined *Atg5*^{+/-} mice for goblet cell abnormalities. Remarkably, even partial deficiency of autophagy signaling (the homozygous mice are embryonically lethal) fully recapitulated the phenotype of mucus layer impairment, goblet cell hyperplasia, and secretory defects (Figures 7A–7D), substantiating the role of

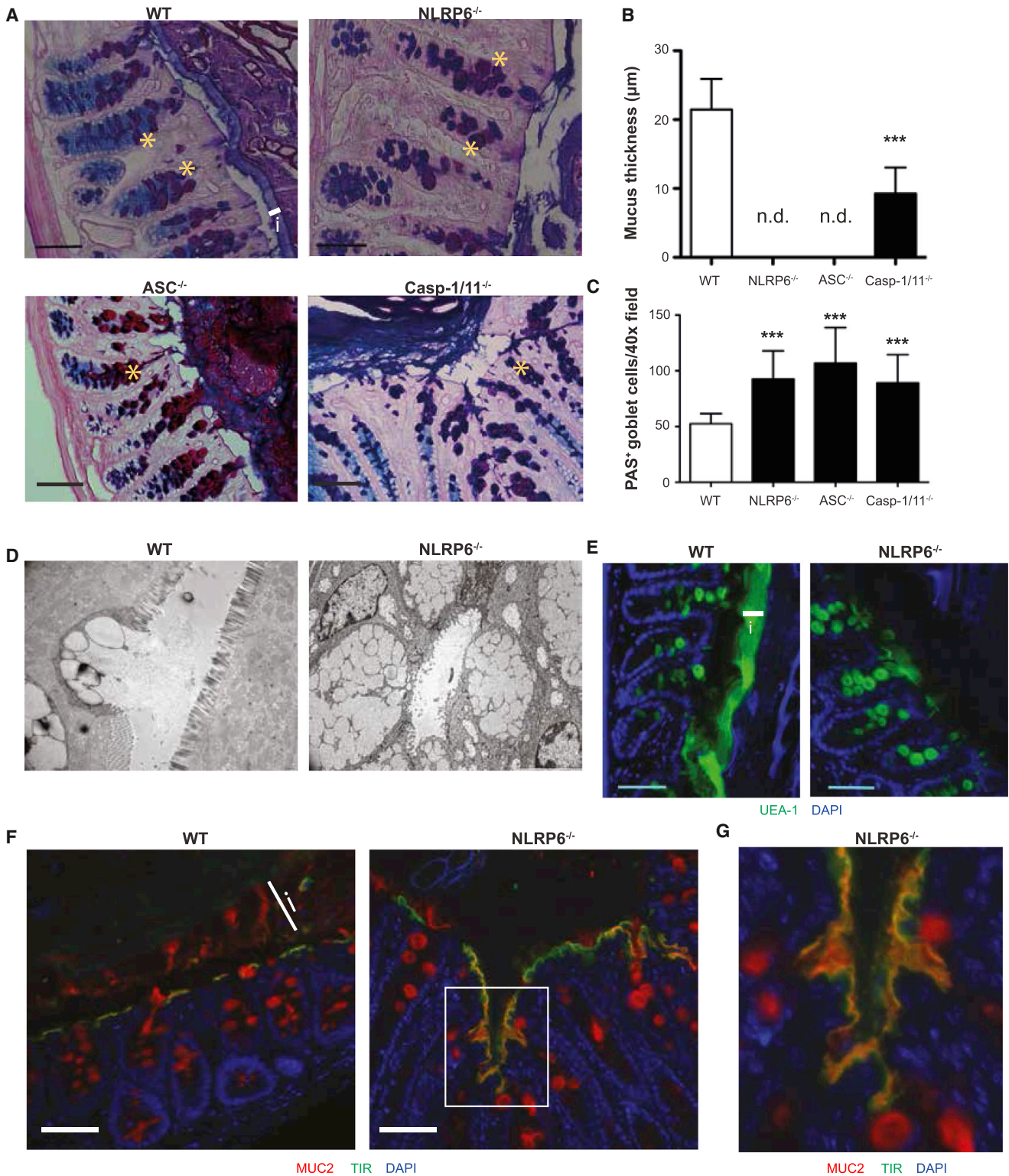


Figure 4. NLRP6 Inflammasome Activity Is Required for Goblet Cell Function and Protection from *C. rodentium* Invasiveness
 (A) AB/PAS stained distal colon sections of WT, *Nlrp6*^{-/-}, *Asc*^{-/-}, and *Caspase-1/11*^{-/-} mice showing the inner mucus layer (i) and goblet cells (asterisks). Magnification = 400×. The scale bar represents 50 μm.
 (B) Quantification of inner mucus layer thickness in the distal colon. The inner mucus layer is absent in *Nlrp6*^{-/-} and *Asc*^{-/-} mice and significantly thinner in *Caspase-1/11*^{-/-} mice, n = 8, 4, and 5 mice, respectively. Significance determined using two-tailed Student's t test and expressed as the mean ± SD (**p < 0.0001).
 (legend continued on next page)

autophagy downstream of inflammasome signaling as a driver of goblet cell secretory function.

DISCUSSION

This report describes an immune mechanism regulating mucin granule exocytosis by goblet cells in the large intestine and identifies the NLRP6 inflammasome as a major mediator of this process. NLRP6 control of mucus secretion directly affects its ability to regulate intestinal and microbial homeostasis while creating a protective niche from enteric pathogens. Genetic deletion of NLRP6 and key components of the inflammasome signaling pathway, caspase-1 and ASC, leads to abrogated mucus secretion characterized by protruding mucin granules, that rather than fusing into the apical basement membrane and releasing their content, are sloughed off into the intestinal lumen in their entirety. We demonstrate that NLRP6 is important in maintaining autophagy in the intestinal epithelium, a process previously shown to be critically important in intestinal granule exocytosis pathway.

NLRP6 is highly expressed in the intestinal epithelium, specifically locating to apical regions surrounding the theca of mature goblet cells. We have not found evidence of NLRP6 mRNA expression in the submucosal colonic region, including myofibroblasts (Normand et al., 2011). Inflammasome signaling has classically been shown to mediate its immune functions through the production of proinflammatory cytokines, although there is recent supporting evidence that inflammasome function is also important in the biological function of a cell beyond IL-1 β and IL-18 production. As an example, caspase-1/inflammasome signaling is essential in adipocyte differentiation and influencing insulin resistance in these cells (Stienstra et al., 2010). Indeed, our findings point toward an IL-1-independent and IL-18-independent goblet cell intrinsic function of inflammasomes in regulating granule secretion. Nevertheless, both cytokines may still play key roles in the orchestration of multiple host-microbiota and inflammatory protective mucosal responses that may integrate with the cytokine-independent inflammasome roles described herein in shaping the host responses to its environment. The specific function of IL-1 and IL-18 in contributing to the overall roles mediated by intestinal inflammasomes thus merits further studies.

As of yet, there have been only very few studies exploring the immune pathways that regulate mucus secretion (Songhet et al., 2011). In NLRP6-deficient mice, the lack of mucus secretion and inability to form an adherent, continuous inner mucus layer enables close microbe-epithelium interactions, and provides an explanation for our previously described observation that the

dysbiotic microbiota in *Nlrp6*^{-/-} mice is intimately associated with the mucosa (Elinav et al., 2011b). This impaired host-microbial interface leads to context-dependent consequences that may include transcriptional epithelial cell reprogramming of CCL5 (Elinav et al., 2011b), influx of bacterial products into the portal circulation upon dietary induction of the metabolic syndrome (Henao-Mejia et al., 2012), and promotion of the IL-6 signaling pathway during inflammation-induced cancer (Hu et al., 2013). As such, the combination of environment (mediating compositional and functional microbial alterations) and genetics (mediating mucus barrier defects through NLRP6 inflammasome deficiency), jointly drive compound “multifactorial” phenotypes such as colonic auto-inflammation, nonalcoholic steatohepatitis (NASH), and inflammation-induced cancer (Chen et al., 2011; Henao-Mejia et al., 2012; Normand et al., 2011). The same alteration in the host-microbial interface may alternatively result in exacerbated infection when a pathogen, such as *C. rodentium* or its human correlate Enteropathogenic *E. Coli*, are introduced into the ecosystem. Therefore, we propose a unified model explaining how host genetic variability (manifested as susceptibility traits in some individuals) coupled with distinct environmental insults may result in seemingly unrelated and variable phenotypic consequences. In human inflammatory bowel disease, as one example, such a model may explain the wide variability in clinical manifestations, even in the lifespan of individual patients, as a variety of intestinal and extra-intestinal auto-inflammatory manifestations, susceptibility to certain infections and a tendency for neoplastic transformation (Grivnikov et al., 2010).

Autophagy has been characterized as being crucial in maintaining the integrity of the Paneth cell granule exocytosis pathway (Cadwell et al., 2008). Deficiency in Atg16L1 led to decreased number and disorganized granules, decreased lysozyme secretion, intact granules present in the crypt lumen, and an abundance of degenerating mitochondria. Likewise in our system, we could visualize formation of autophagosomes in the intestinal epithelium, including within goblet cells, and to demonstrate that NLRP6-deficient epithelium lacked visible autophagosome formation and an altered LC3I/II ratio. This suggests that the activity of the NLRP6 inflammasome is critical for autophagy induction and activity in the intestinal epithelium. Corresponding to a reduction in the activity of autophagy in the intestine of *Nlrp6*^{-/-} mice, there was an accumulation of p62 and an abundance of degenerating mitochondria, both targets of autophagy for degradation. Given the important function of autophagy in numerous secretory pathways (Cadwell et al., 2008; DeSelm et al., 2011; Ushio et al., 2011), it is likely that the mechanism whereby NLRP6 deficiency leads to defective

(C) Quantification of goblet cell number in the distal colon. *Nlrp6*^{-/-} (**p = 0.0001), *Asc*^{-/-} (**p = 0.0001), and *Caspase1/11*^{-/-} (**p = 0.0007) mice exhibit goblet cell hyperplasia, n = 8, 4, and 5 mice, respectively.

(D) Representative transmission electron microscopy images taken from colonic sections of WT mice and *Nlrp6*^{-/-} mice, n = 4 mice per group.

(E) Representative epifluorescence staining for mucus using the lectin UEA-1 (green) with DAPI (blue) as a counter stain. The inner mucus layer is absent in *Nlrp6*^{-/-} mice. i, inner mucus layer. Original magnification = 200 \times . The scale bar represents 50 μ m.

(F) Representative immunostaining for the *C. rodentium* effector Tir (green) and the mucus-specific protein Muc2 (red) in colon, with DAPI (blue) as a counter stain, in WT and *Nlrp6*^{-/-} mice at 7 days p.i. The inner mucus layer is visible in WT mice and is lacking in the *Nlrp6*^{-/-} mice. Magnification = 200 \times . The scale bar represents 50 μ m.

(G) In *Nlrp6*^{-/-} mice, *C. rodentium* (green) appears to be more invasive, as shown by deeper penetration into the crypts, which often colocalizes with Muc2 (red). See also Figures S2 and S3.

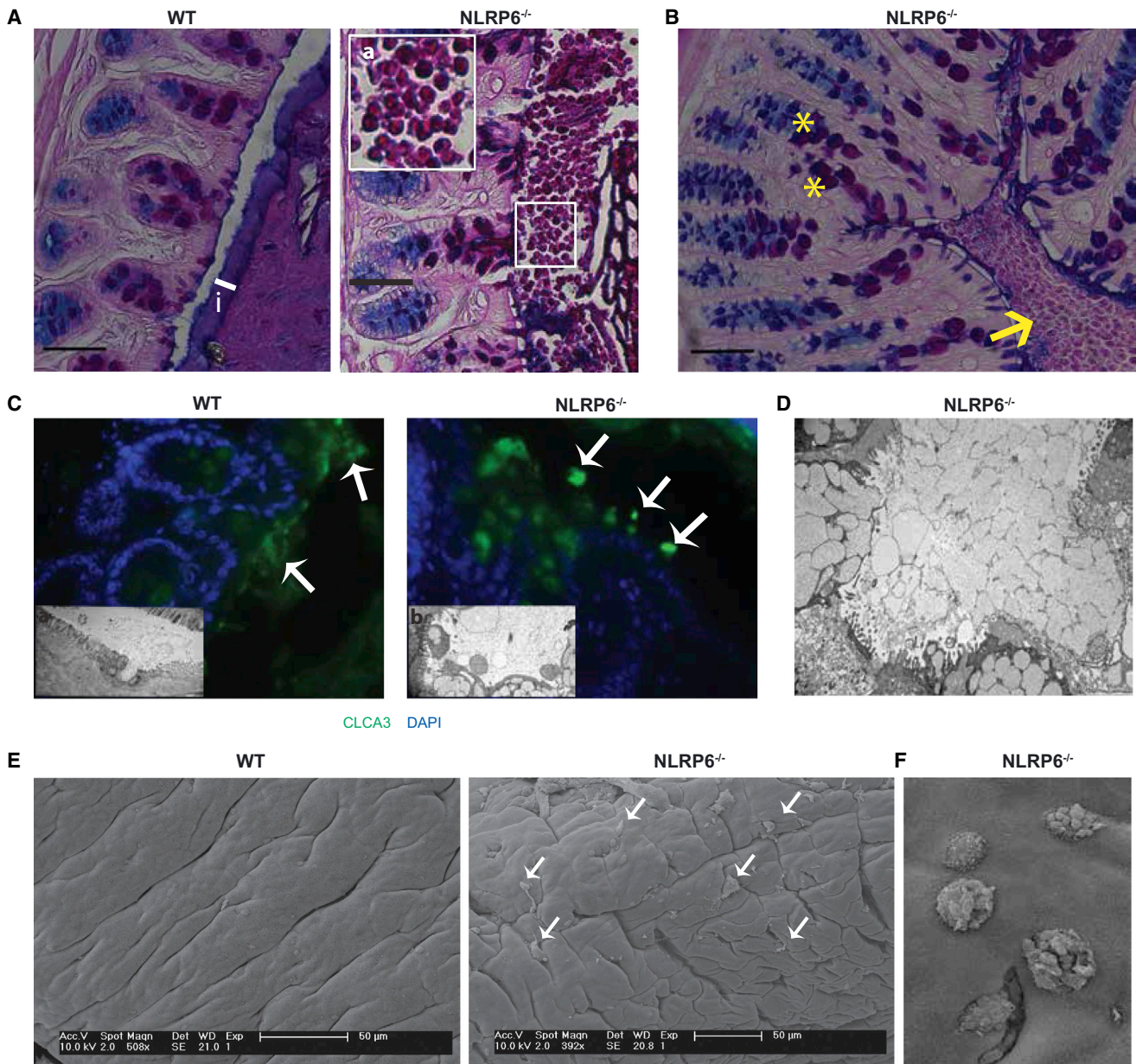


Figure 5. NLRP6 Inflammasome Is Required for Mucus Granule Exocytosis

(A) Representative AB/PAS-stained colon sections showing the inner mucus layer (i) in WT mice. *Nlrp6*^{-/-} mice show the presence of granule-like structures within the lumen (inset a). The scale bar represents 50 μ m.

(B) AB/PAS-stained *Nlrp6*^{-/-} distal colon section showing accumulation of mucin granule-like structures in the lumen (arrowhead) and an increased number of large PAS⁺ goblet cells (asterisks). The scale bar represents 50 μ m.

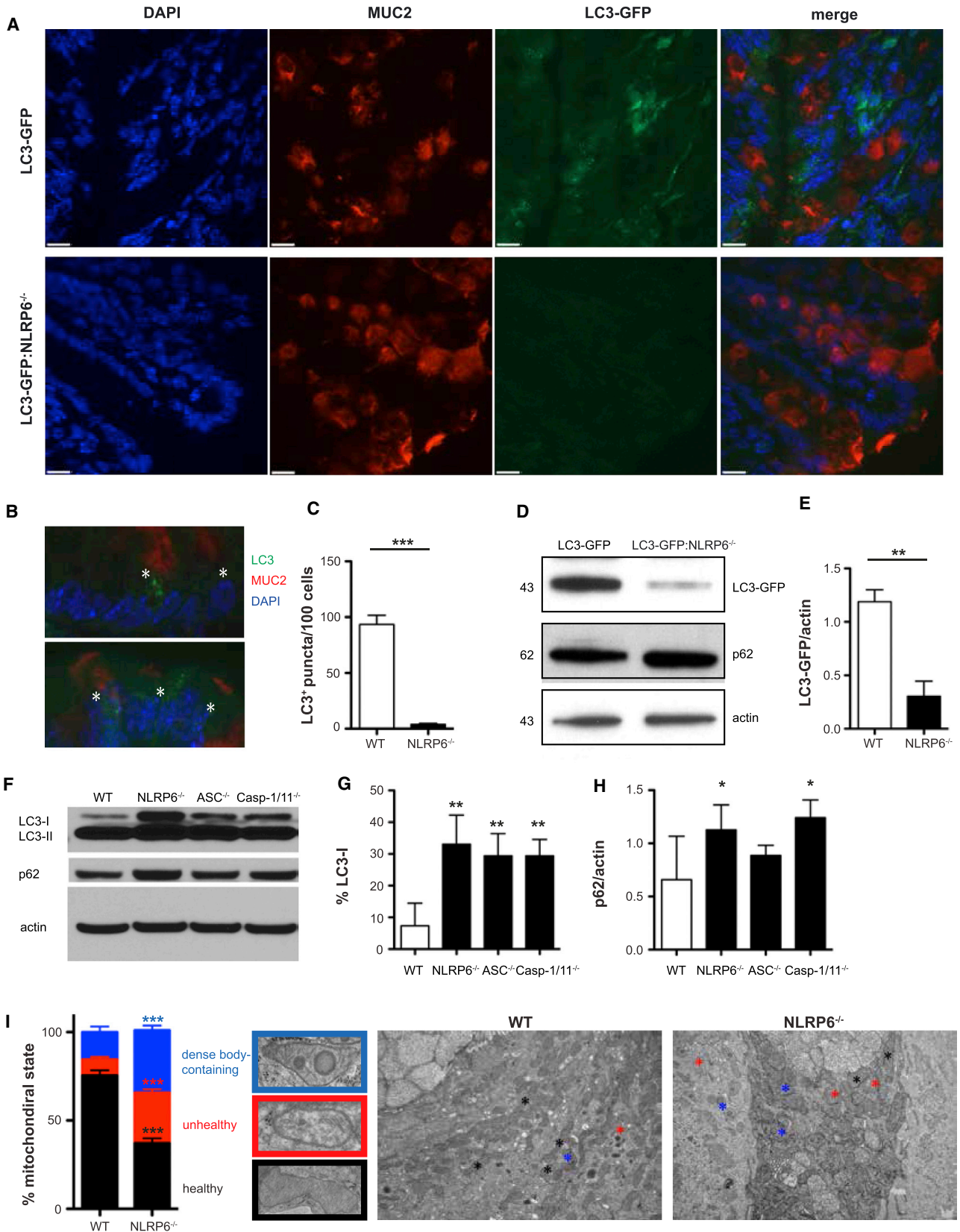
(C) Representative immunostaining for the goblet cell-specific protein, Clca3 (green), with DAPI (blue) as a counter stain in distal colon sections. Arrowheads show diffuse staining of Clca3 in the WT lumen and punctate staining in the *Nlrp6*^{-/-} lumen. Representative transmission electron microscopy images (insets a and b) show intact mucus secretion by a goblet cell in WT and dysfunctional mucus granule exocytosis and the presence of granule-like structures in *Nlrp6*^{-/-} distal colon tissue.

(D) Transmission electron microscopy image of the *Nlrp6*^{-/-} distal colon showing protrusion of mucin granules into the lumen without mucus secretion and intact mucin granules saturating the intestinal lumen, n = 4 mice.

(E) Representative scanning electron microscopy images of the distal colon of WT and *Nlrp6*^{-/-} mice, n = 2 mice per group. Each experiment was repeated three times. A smooth intestinal epithelium is seen in WT mice. A large number of goblet cells with mucin granules protruding into the lumen (arrowheads) are seen in *Nlrp6*^{-/-} mice.

(F) Enlarged scanning electron microscopy image of four goblet cells with protruding mucin granules into the *Nlrp6*^{-/-} intestinal lumen.

See also Figure S4.



(legend on next page)

mucus granule exocytosis is by inhibiting the autophagic processes required for proper secretion of mucus granules. Such autophagy-induced regulation of goblet cell secretory functions was recently demonstrated to involve downstream reactive oxygen species signaling (Patel et al., 2013).

Colonizing the outer mucus layer and penetrating the inner mucus layer is a key step in the pathogenesis of *C. rodentium* and is likely achieved by the production of virulence factors with mucinase activity (Bergstrom et al., 2010). Further, goblet cell-driven mucus secretion has been shown to be critical in resolving *C. rodentium* infection by dissociating adherent *C. rodentium* from the intestinal mucosa (Bergstrom et al., 2008, 2010). Likewise, in our study, increased susceptibility to *C. rodentium* in *Nlrp6*^{-/-} mice is a consequence of the lack of an inner mucus layer and abrogated mucus secretion in the NLRP6-deficient mucosa. Further, NLRP6-mediated defense against this mucosal pathogen is dependent on inflammasome assembly, as deficiency in ASC and caspase-1 all resulted in increased *C. rodentium* burdens late in infection. Notably, other NLRP6 regulatory effects may contribute to containment of intestinal infection, such as those mediated by regulation of microbiota composition, recently highlighted to be central in regulation of *C. rodentium* clearance (Kamada et al., 2012).

A recent study has shown increased resistance of *Nlrp6*^{-/-} mice to systemically administered bacterial pathogens, including *Listeria monocytogenes*, *Salmonella* Typhimurium, and *Escherichia coli* (Anand et al., 2012). These results probably stem from differences in systemic versus local host-related mechanisms of innate immune protection against invading pathogens. In a systemic bacterial infection, myeloid cells in circulation would be the primary responders to infection whereas in an intestinal bacterial infection epithelial cells would be involved in pathogen detection. It is not without precedence that inflammasome sensors have seemingly opposing function depending on

the cell type involved, with important differences in hematopoietic cells versus nonhematopoietic cells for the NLRP6 inflammasome characterized (Anand et al., 2012; Chen et al., 2011). Notably, the alteration in the mucosal antipathogenic immune response may be accompanied by a compensatory hyperactive systemic immune response, providing yet another example of the plasticity and rapid adoptability of the seemingly “primitive” innate immune arm (Slack et al., 2009).

Our study reveals the importance of the NLRP6 inflammasome in mucus granule exocytosis, showing the relevance of inflammasome signaling in initiation of autophagy and maintaining goblet cell function. It suggests that goblet cells, previously regarded as passive contributors to the formation of the biophysical protective mucosal layers, may be actually active, regulatory hubs integrating signals from the host and its environment as an integral component of the innate immune response. Further mechanistic studies to assess the ligands for the NLRP6 inflammasome and how it may coordinate autophagy and the mucus-granule exocytosis pathway are of significant interest, as they impact greatly on host microbial interactions at mucosal interfaces.

EXPERIMENTAL PROCEDURES

A detailed description of materials and methods used in this paper can be found in the [Supplemental Information](#).

Mice

NLRP6^{-/-} (Elinav et al., 2011b), *ASC*^{-/-} (Sutterwala et al., 2006), *Casp1*^{-/-} (Kuida et al., 1995), *Atg5*^{+/-}, *IL-1R*^{-/-}, and *IL-18*^{-/-} (Takeda et al., 1998) mice were described in previous publications. All animal experimentation was approved by an institutional animal care and use committee (IACUC).

Bacterial Strains and Infection of Mice

Mice were infected by oral gavage with 0.1 ml of an overnight culture of LB containing approximately 1 × 10⁹ colony-forming units (cfu) of a

Figure 6. NLRP6 Is Required for Autophagosome Formation in the Intestinal Epithelium

- (A) Representative immunofluorescence image of WT (LC3, top panel) and NLRP6-deficient (LC3: *Nlrp6*^{-/-}, bottom panel) intestinal epithelium shows abrogated autophagy in the absence of NLRP6. Goblet cells are stained with the mucus-specific protein Muc2 (red), epithelial cell nuclei are indicated with DAPI (blue). Formation of autophagosomes is visualized utilizing the LC3-GFP endogenously expressed protein (green). The scale bar represents 70 μm.
- (B) Magnification of intestinal epithelial cells showing WT goblet cells (Muc2 positive; red) active in the formation of autophagosomes, seen as punctate staining with the LC3-GFP endogenous protein colocalizing with Muc2-positive cells.
- (C) Quantitation of autophagosome formation through enumeration of LC3 puncta per 100 epithelial cells, n = 5 mice per group. Significance determined using two-tailed Student's t test and expressed as the mean ± SEM (**p < 0.0001).
- (D) Immunoblot analysis of total LC3-GFP, and p62 proteins in isolated intestinal epithelial cells from WT LC3-GFP transgenic mice and NLRP6-deficient GFP-LC3 transgenic mice.
- (E) LC3-GFP band intensities from (D) were quantified and normalized to actin band intensity, n = 5 mice per group. Significance determined using two-tailed Student's t test and expressed as the mean ± SEM (**p = 0.0067).
- (F) Immunoblot analysis of total endogenous LC3-I/II and p62 proteins in isolated intestinal epithelial cells of WT, *Nlrp6*^{-/-}, *Asc*^{-/-}, and *Caspase-1/11*^{-/-} mice. LC3-I and LC3-II denote the nonlipidated (cytosolic) and lipidated (autophagosome membrane) forms of LC3, respectively.
- (G) Accumulation of LC3-I in isolated epithelial cells from *Nlrp6*^{-/-} (**p = 0.0015), *Asc*^{-/-} (**p = 0.0013), and *Caspase-1/11*^{-/-} (**p = 0.0025) mice, as shown by the fraction of LC3-I band density out of total LC3 band density. Data represent n = 6 (WT, *Nlrp6*^{-/-}, and *Asc*^{-/-} mice) or n = 4 (*Caspase-1/11*^{-/-} mice). Significance determined using two-tailed Student's t test and expressed as the mean ± SD.
- (H) Increased abundance of p62 in *Nlrp6*^{-/-} (p = 0.0349), *Asc*^{-/-} (ns, p = 0.2115), and *Caspase-1/11*^{-/-} (p = 0.0284) mice, as shown by quantification of p62 band intensity. Data represent n = 6 (WT, *Nlrp6*^{-/-}, and *Asc*^{-/-} mice) or n = 4 (*Caspase-1/11*^{-/-} mice). Significance determined using two-tailed Student's t test and expressed as the mean ± SD.
- (I) Mitochondria were scored and enumerated in WT and *Nlrp6*^{-/-} intestinal epithelial cells as healthy (black), unhealthy (red) and dense inclusion body containing (blue), n = 25 or 28 epithelial cells, respectively. Mitochondrial dysfunction was characterized in *Nlrp6*^{-/-} mice as a decrease in total healthy mitochondria (**p < 0.0001) and an accumulation of unhealthy (**p < 0.0001) and dense inclusion body-containing (**p = 0.0002) mitochondria. Significance determined using two-tailed Student's t test and expressed as the mean ± SEM. Representative transmission electron microscopy images are shown (magnification = 11,500×) and healthy (black asterisk), unhealthy (red asterisk), and dense inclusion body containing (blue asterisk) mitochondria are depicted within WT and *Nlrp6*^{-/-} intestinal epithelial cells.

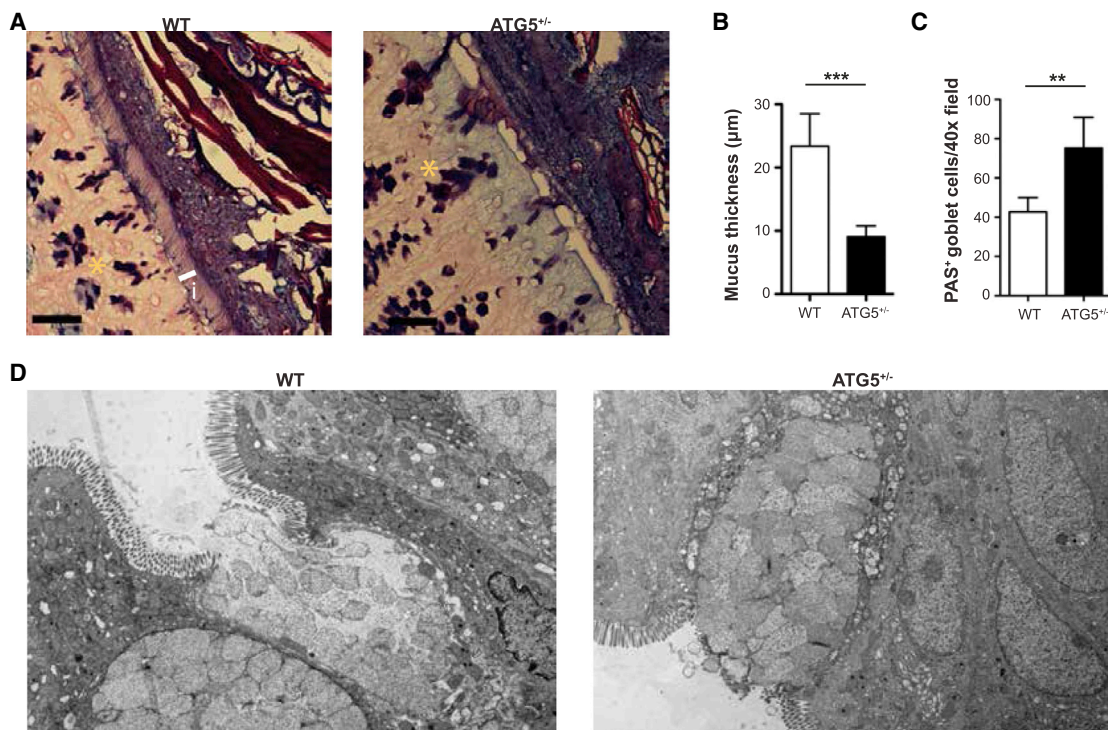


Figure 7. Autophagy Is Required for Goblet Cell Function and Mucus Secretion in the Intestine

(A) Representative AB/PAS-stained colon sections showing the inner mucus layer (i) in WT mice. *Atg5* heterozygous mice show reduced production of the inner mucus layer and goblet cell hyperplasia (asterisk). The scale bar represents 50 μm.

(B) Quantification of inner mucus layer thickness in the distal colon. The inner mucus layer is significantly thinner in the *Atg5*^{+/-} distal colon, *n* = 3 mice. Significance determined using two-tailed Student's *t* test and expressed as the mean ± SD (***p* < 0.0001).

(C) Quantification of goblet cell number in the distal colon. *Atg5*^{+/-} mice exhibit goblet cell hyperplasia, *n* = 3 mice. Significance determined using two-tailed Student's *t* test and expressed as the mean ± SD (***p* = 0.0030).

(D) Transmission electron microscopy image of *Atg5*^{+/-} showing reduced mucus secretion. Theca of WT mice fuse with surface of epithelium resulting in mucus granule shedding and release of contained mucins. Fusion and granule release is stalled in *Atg5*^{+/-} mice.

kanamycin-resistant, luciferase-expressing derivative of *C. rodentium* DBS100 (ICC180) and analyzed on day 15 postinfection, unless otherwise stated.

Transmission and Scanning Electron Microscopy

Selected tissues were fixed in 2.5% glutaraldehyde in 0.1 M sodium cacodylate buffer pH 7.4 for 1–2 hr. Samples were rinsed three times in sodium cacodylate buffer and postfixed in 1% osmium tetroxide for 1 hr, en bloc stained in 2% uranyl acetate in maleate buffer pH 5.2 for a further hour, then rinsed, dehydrated, infiltrated with Epon812 resin, and baked overnight at 60°C. Hardened blocks were cut using a Leica UltraCut UCT. Sixty nanometer thick sections were collected and stained using 2% uranyl acetate and lead citrate. Samples were all viewed in an FEI Tencai Biotwin TEM at 80 kV. Images were taken using Morada CCD and iTEM (Olympus) software.

Goblet Cell and Mucus Layer Preservation Ex Vivo

The terminal 5 mm of the colon were excised, immediately submerged in Ethanol-Carnoy's Fixative at 4°C for 2 hr and then placed into 100% ethanol. Fixed colon tissues were embedded in paraffin and cut into 5 μm sections. Tissues were stained with Alcian blue/PAS.

Statistical Analysis

Statistical significance was calculated by using a two-tailed Student's *t* test unless otherwise stated, with assistance from GraphPad Prism Software Version 4.00 (GraphPad Software). If not otherwise specified, statistical significance was given as ****p* value < 0.0001; ***p* value < 0.005; **p* value < 0.05; ns

(not significant); *p* value > 0.05. The results are expressed as the mean value with SEM unless otherwise indicated.

SUPPLEMENTAL INFORMATION

Supplemental Information includes Extended Experimental Procedures and four figures and can be found with this article online at <http://dx.doi.org/10.1016/j.cell.2014.01.026>.

AUTHOR CONTRIBUTIONS

M.W. performed experiments, interpreted the results, and participated in writing the manuscript. C.A.T. and R.N. contributed multiple experiments, participated in writing the manuscript and equally contributed to the project as second authors. J.H.M., J.Z., M.L., M.N.K., and W.M.P. contributed multiple in vivo and ex vivo experiments and participated in the editing of the manuscript. GF contributed meaningful insights to the *C. rodentium* experiments in this study, performed with bioluminescent bacteria that he generated. E.E., B.B.F., and R.A.F. equally contributed to the study as they conceived the project, mentored and supervised its participants, interpreted its results, and wrote the manuscript.

ACKNOWLEDGMENTS

We thank the members of the Elinav, Finlay, and Flavell labs and Zamir Halpern, Tel Aviv Sourasky Medical Center, for fruitful scientific discussions. We

thank Akiko Iwasaki, Yale University School of Medicine, for kindly providing LC3 reporter mice. We thank the Weizmann Institute management and Alon Harmelin, director of the Department of Veterinary Resources, for providing financial and infrastructural support. We thank M. Graham and X. Liu, CCMI EM Core Facility, Yale School of Medicine. M.W. is supported through the Canadian Institutes of Health Research (CIHR) doctoral award-Frederick Banting and Charles Best Canada graduate scholarship. C.A.T. is the recipient of a Boehringer Ingelheim Fonds PhD Fellowship. M.N.K. was supported by a travel grant from the Friends of Tel Aviv Sourasky Medical Center Foundation. E.E. is supported by Yael and Rami Ungar, Israel, Abisch Frenkel Foundation for the Promotion of Life Sciences, the Gurwin Family Fund for Scientific Research, Leona M. and Harry B. Helmsley Charitable Trust, Crown Endowment Fund for Immunological Research, Estate of Jack Gitlitz, Estate of Lydia Hershkovich, grants funded by the European Research Council, the Kenneth Rainin Foundation, the German-Israel Bination Foundation, the Israel Science Foundation, the Minerva Foundation, and the Alon Foundation scholar award. B.B.F. is supported by operating grants from CIHR and is the UBC Peter Wall Distinguished Professor. R.A.F. is supported by grants from the US Department of Defense and the Blavatnik Family Foundation and is a Howard Hughes Medical Institute (HHMI) investigator.

Received: July 19, 2013

Revised: November 12, 2013

Accepted: January 10, 2014

Published: February 27, 2014

REFERENCES

- Ambort, D., Johansson, M.E., Gustafsson, J.K., Nilsson, H.E., Ermund, A., Johansson, B.R., Koeck, P.J., Hebert, H., and Hansson, G.C. (2012). Calcium and pH-dependent packing and release of the gel-forming MUC2 mucin. *Proc. Natl. Acad. Sci. USA* *109*, 5645–5650.
- Anand, P.K., Malireddi, R.K., Lukens, J.R., Vogel, P., Bertin, J., Lamkanfi, M., and Kanneganti, T.D. (2012). NLRP6 negatively regulates innate immunity and host defence against bacterial pathogens. *Nature* *488*, 389–393.
- Artis, D., Wang, M.L., Keilbaugh, S.A., He, W., Brenes, M., Swain, G.P., Knight, P.A., Donaldson, D.D., Lazar, M.A., Miller, H.R., et al. (2004). RELMbeta/FIZZ2 is a goblet cell-specific immune-effector molecule in the gastrointestinal tract. *Proc. Natl. Acad. Sci. USA* *101*, 13596–13600.
- Bergstrom, K.S., Guttman, J.A., Rumi, M., Ma, C., Bouzari, S., Khan, M.A., Gibson, D.L., Vogl, A.W., and Vallance, B.A. (2008). Modulation of intestinal goblet cell function during infection by an attaching and effacing bacterial pathogen. *Infect. Immun.* *76*, 796–811.
- Bergstrom, K.S., Kisooson-Singh, V., Gibson, D.L., Ma, C., Montero, M., Sham, H.P., Ryz, N., Huang, T., Velcich, A., Finlay, B.B., et al. (2010). Muc2 protects against lethal infectious colitis by disassociating pathogenic and commensal bacteria from the colonic mucosa. *PLoS Pathog.* *6*, e1000902.
- Cadwell, K., Liu, J.Y., Brown, S.L., Miyoshi, H., Loh, J., Lennerz, J.K., Kishi, C., Kc, W., Carrero, J.A., Hunt, S., et al. (2008). A key role for autophagy and the autophagy gene Atg16l1 in mouse and human intestinal Paneth cells. *Nature* *456*, 259–263.
- Chen, G.Y., Liu, M., Wang, F., Bertin, J., and Núñez, G. (2011). A functional role for Nlrp6 in intestinal inflammation and tumorigenesis. *J. Immunol.* *186*, 7187–7194.
- Choi, A.M., Ryter, S.W., and Levine, B. (2013). Autophagy in human health and disease. *N. Engl. J. Med.* *368*, 1845–1846.
- DeSelm, C.J., Miller, B.C., Zou, W., Beatty, W.L., van Meel, E., Takahata, Y., Klumperman, J., Tooze, S.A., Teitelbaum, S.L., and Virgin, H.W. (2011). Autophagy proteins regulate the secretory component of osteoclastic bone resorption. *Dev. Cell* *21*, 966–974.
- Elinav, E., Strowig, T., Henao-Mejia, J., and Flavell, R.A. (2011a). Regulation of the antimicrobial response by NLR proteins. *Immunity* *34*, 665–679.
- Elinav, E., Strowig, T., Kau, A.L., Henao-Mejia, J., Thaïss, C.A., Booth, C.J., Peaper, D.R., Bertin, J., Eisenbarth, S.C., Gordon, J.I., and Flavell, R.A. (2011b). NLRP6 inflammasome regulates colonic microbial ecology and risk for colitis. *Cell* *145*, 745–757.
- Elinav, E., Henao-Mejia, J., and Flavell, R.A. (2013a). Integrative inflammatory activity in the regulation of intestinal mucosal immune responses. *Mucosal Immunol.* *6*, 4–13.
- Elinav, E., Thaïss, C.A., and Flavell, R.A. (2013b). Analysis of microbiota alterations in inflammasome-deficient mice. *Methods Mol. Biol.* *1040*, 185–194.
- Forstner, G. (1995). Signal transduction, packaging and secretion of mucins. *Annu. Rev. Physiol.* *57*, 585–605.
- Gill, N., Wlodarska, M., and Finlay, B.B. (2011). Roadblocks in the gut: barriers to enteric infection. *Cell. Microbiol.* *13*, 660–669.
- Grenier, J.M., Wang, L., Manji, G.A., Huang, W.J., Al-Garawi, A., Kelly, R., Carlson, A., Merriam, S., Lora, J.M., Briskin, M., et al. (2002). Functional screening of five PYPAF family members identifies PYPAF5 as a novel regulator of NF- κ B and caspase-1. *FEBS Lett.* *530*, 73–78.
- Grivnennikov, S.I., Greten, F.R., and Karin, M. (2010). Immunity, inflammation, and cancer. *Cell* *140*, 883–899.
- Henao-Mejia, J., Elinav, E., Jin, C., Hao, L., Mehal, W.Z., Strowig, T., Thaïss, C.A., Kau, A.L., Eisenbarth, S.C., Jurczak, M.J., et al. (2012). Inflammasome-mediated dysbiosis regulates progression of NAFLD and obesity. *Nature* *482*, 179–185.
- Henao-Mejia, J., Elinav, E., Thaïss, C.A., and Flavell, R.A. (2013a). The intestinal microbiota in chronic liver disease. *Adv. Immunol.* *117*, 73–97.
- Henao-Mejia, J., Elinav, E., Thaïss, C.A., Licona-Limon, P., and Flavell, R.A. (2013b). Role of the intestinal microbiome in liver disease. *J. Autoimmun.* *46*, 66–73.
- Hu, B., Elinav, E., Huber, S., Strowig, T., Hao, L., Hafemann, A., Jin, C., Wunderlich, C., Wunderlich, T., Eisenbarth, S.C., and Flavell, R.A. (2013). Microbiota-induced activation of epithelial IL-6 signaling links inflammasome-driven inflammation with transmissible cancer. *Proc. Natl. Acad. Sci. USA* *110*, 9862–9867.
- Inoue, J., Nishiumi, S., Fujishima, Y., Masuda, A., Shiomi, H., Yamamoto, K., Nishida, M., Azuma, T., and Yoshida, M. (2012). Autophagy in the intestinal epithelium regulates *Citrobacter rodentium* infection. *Arch. Biochem. Biophys.* *521*, 95–101.
- Johansson, M.E., Phillipson, M., Petersson, J., Velcich, A., Holm, L., and Hansson, G.C. (2008). The inner of the two Muc2 mucin-dependent mucus layers in colon is devoid of bacteria. *Proc. Natl. Acad. Sci. USA* *105*, 15064–15069.
- Kamada, N., Kim, Y.G., Sham, H.P., Vallance, B.A., Puente, J.L., Martens, E.C., and Núñez, G. (2012). Regulated virulence controls the ability of a pathogen to compete with the gut microbiota. *Science* *336*, 1325–1329.
- Kuida, K., Lippke, J.A., Ku, G., Harding, M.W., Livingston, D.J., Su, M.S., and Flavell, R.A. (1995). Altered cytokine export and apoptosis in mice deficient in interleukin-1 beta converting enzyme. *Science* *267*, 2000–2003.
- Leverkoehne, I., and Gruber, A.D. (2002). The murine mCLCA3 (alias gob-5) protein is located in the mucin granule membranes of intestinal, respiratory, and uterine goblet cells. *J. Histochem. Cytochem.* *50*, 829–838.
- Linden, S.K., Sutton, P., Karlsson, N.G., Korolik, V., and McGuckin, M.A. (2008). Mucins in the mucosal barrier to infection. *Mucosal Immunol.* *1*, 183–197.
- Lupp, C., Robertson, M.L., Wickham, M.E., Sekirov, I., Champion, O.L., Gaynor, E.C., and Finlay, B.B. (2007). Host-mediated inflammation disrupts the intestinal microbiota and promotes the overgrowth of Enterobacteriaceae. *Cell Host Microbe* *2*, 204.
- Mizushima, N., Yamamoto, A., Matsui, M., Yoshimori, T., and Ohsumi, Y. (2004). In vivo analysis of autophagy in response to nutrient starvation using transgenic mice expressing a fluorescent autophagosome marker. *Mol. Biol. Cell* *15*, 1101–1111.
- Nair, M.G., Guild, K.J., Du, Y., Zaph, C., Yancopoulos, G.D., Valenzuela, D.M., Murphy, A., Stevens, S., Karow, M., and Artis, D. (2008). Goblet cell-derived resistin-like molecule beta augments CD4+ T cell production of IFN- γ and infection-induced intestinal inflammation. *J. Immunol.* *181*, 4709–4715.
- Normand, S., Delanoye-Crespin, A., Bressenot, A., Huot, L., Grandjean, T., Peyrin-Biroulet, L., Lemoine, Y., Hot, D., and Chamaillard, M. (2011). Nod-like receptor pyrin domain-containing protein 6 (NLRP6) controls epithelial

- self-renewal and colorectal carcinogenesis upon injury. *Proc. Natl. Acad. Sci. USA* *108*, 9601–9606.
- Patel, K.K., Miyoshi, H., Beatty, W.L., Head, R.D., Malvin, N.P., Cadwell, K., Guan, J.L., Saitoh, T., Akira, S., Seglen, P.O., et al. (2013). Autophagy proteins control goblet cell function by potentiating reactive oxygen species production. *EMBO J.* *32*, 3130–3144.
- Rodríguez-Piñero, A.M., van der Post, S., Johansson, M.E., Thomsson, K.A., Nesvizhskii, A.I., and Hansson, G.C. (2012). Proteomic study of the mucin granulae in an intestinal goblet cell model. *J. Proteome Res.* *11*, 1879–1890.
- Slack, E., Hapfelmeier, S., Stecher, B., Velykoredko, Y., Stoel, M., Lawson, M.A., Geuking, M.B., Beutler, B., Tedder, T.F., Hardt, W.D., et al. (2009). Innate and adaptive immunity cooperate flexibly to maintain host-microbiota mutualism. *Science* *325*, 617–620.
- Songhet, P., Barthel, M., Stecher, B., Müller, A.J., Kremer, M., Hansson, G.C., and Hardt, W.D. (2011). Stromal IFN- γ R-signaling modulates goblet cell function during *Salmonella* Typhimurium infection. *PLoS ONE* *6*, e22459.
- Stecher, B., Robbiani, R., Walker, A.W., Westendorf, A.M., Barthel, M., Kremer, M., Chaffron, S., Macpherson, A.J., Buer, J., Parkhill, J., et al. (2007). *Salmonella enterica* serovar typhimurium exploits inflammation to compete with the intestinal microbiota. *PLoS Biol.* *5*, 2177–2189.
- Stienstra, R., Joosten, L.A., Koenen, T., van Tits, B., van Diepen, J.A., van den Berg, S.A., Rensen, P.C., Voshol, P.J., Fantuzzi, G., Hijmans, A., et al. (2010). The inflammasome-mediated caspase-1 activation controls adipocyte differentiation and insulin sensitivity. *Cell Metab.* *12*, 593–605.
- Sutterwala, F.S., Ogura, Y., Szczepanik, M., Lara-Tejero, M., Lichtenberger, G.S., Grant, E.P., Bertin, J., Coyle, A.J., Galán, J.E., Askenase, P.W., and Flavell, R.A. (2006). Critical role for NALP3/CIAS1/Cryopyrin in innate and adaptive immunity through its regulation of caspase-1. *Immunity* *24*, 317–327.
- Takeda, K., Tsutsui, H., Yoshimoto, T., Adachi, O., Yoshida, N., Kishimoto, T., Okamura, H., Nakanishi, K., and Akira, S. (1998). Defective NK cell activity and Th1 response in IL-18-deficient mice. *Immunity* *8*, 383–390.
- Tytgat, K.M., Büller, H.A., Opdam, F.J., Kim, Y.S., Einerhand, A.W., and Dekker, J. (1994). Biosynthesis of human colonic mucin: Muc2 is the prominent secretory mucin. *Gastroenterology* *107*, 1352–1363.
- Ushio, H., Ueno, T., Kojima, Y., Komatsu, M., Tanaka, S., Yamamoto, A., Ichimura, Y., Ezaki, J., Nishida, K., Komazawa-Sakon, S., et al. (2011). Crucial role for autophagy in degranulation of mast cells. *J. Allergy Clin. Immunol.* *127*, 1267–1276.
- van der Sluis, M., De Koning, B.A., De Bruijn, A.C., Velcich, A., Meijerink, J.P., Van Goudoever, J.B., Büller, H.A., Dekker, J., Van Seuningen, I., Renes, I.B., and Einerhand, A.W. (2006). Muc2-deficient mice spontaneously develop colitis, indicating that MUC2 is critical for colonic protection. *Gastroenterology* *131*, 117–129.
- van der Sluis, M., Bouma, J., Vincent, A., Velcich, A., Carraway, K.L., Buller, H.A., Einerhand, A.W., van Goudoever, J.B., Van Seuningen, I., and Renes, I.B. (2008). Combined defects in epithelial and immunoregulatory factors exacerbate the pathogenesis of inflammation: mucin 2-interleukin 10-deficient mice. *Lab. Invest.* *88*, 634–642.
- Wiles, S., Pickard, K.M., Peng, K., MacDonald, T.T., and Frankel, G. (2006). In vivo bioluminescence imaging of the murine pathogen *Citrobacter rodentium*. *Infect. Immun.* *74*, 5391–5396.
- Wysolmerski, J.J., Philbrick, W.M., Dunbar, M.E., Lanske, B., Kronenberg, H., and Broadus, A.E. (1998). Rescue of the parathyroid hormone-related protein knockout mouse demonstrates that parathyroid hormone-related protein is essential for mammary gland development. *Development* *125*, 1285–1294.